CrossMark
click for updates

Characterization of Antibody Bipolar Bridging Mediated by the Human Cytomegalovirus Fc Receptor gp68

Blaise Ndjamen,[a] Devashish S. Joshi,[a] Scott E. Fraser,[b] Pamela J. Bjorkman[a]

Division of Biology and Biological Engineering, California Institute of Technology, Pasadena, California, USA[a]; Translational Imaging Center, University of Southern California, Los Angeles, California, USA[b]

The human cytomegalovirus glycoprotein gp68 functions as an Fc receptor for host IgGs and can form antibody bipolar bridging (ABB) complexes in which gp68 binds the Fc region of an antigen-bound IgG. Here we show that gp68-mediated endocytosis transports ABB complexes into endosomes, after which the complex is routed to lysosomes, presumably for degradation. These results suggest gp68 contributes to evasion of IgG-mediated immune responses by mediating destruction of host IgG and viral antigens.

The betaherpesvirus human cytomegalovirus (HCMV) affects 50 to 98% of people, causing severe symptoms in newborns and a lifetime latent infection that can be lethal in immunocompromised individuals (1). HCMV can also establish recurrent secondary infections after reactivation from latency (2). Immune evasion strategies of herpesviruses include expression of viral Fc receptors (FcγRs) that bind host IgG to evade immune responses mediated by host FcγRs (3–6). Viral FcγRs can participate in antibody bipolar bridging (ABB), whereby an antibody simultaneously binds antigen via its fragment antigen-binding (Fab) arms and an Fc receptor using its Fc (7–9). While there is likely a large excess of nonviral IgG compared with antiviral IgG, the proximity of viral FcγRs to Fc regions from IgGs bound to viral antigens on an infected cell could allow viral FcγRs to preferentially bind antiviral IgGs. ABB protects virally infected cells from antibody- and complement-dependent neutralization (10), antibody-dependent cell-mediated cytotoxicity (11), and granulocyte attachment (12). The HCMV glycoproteins gp68, gp34, Toll-like receptor 12 (TLR12), and TLR13 act as FcγRs to bind human IgG (3, 6, 13, 14). Recent studies reported formation of ABB complexes with gp68 and with gp34 and demonstrated their functional importance by showing that cells infected with HCMV lacking gp68 and/or gp34 triggered stronger activation of the host FcγRs and NK cells than cells infected with wild-type HCMV (15).

In previous studies of ABB, we used cells expressing gE-gI, a herpes simplex virus 1 (HSV-1) FcγR, and gD, an HSV-1 cell surface antigen, to show that anti-gD IgGs formed ABB complexes with gE-gI and gD and that anti-gD IgG and gD were internalized in a gE-gI-dependent process, resulting in lysosomal localization of IgG and gD, but not gE-gI (8) (Fig. 1). Since gE-gI binds Fc at neutral/basic, but not acidic, pH (8, 16), these results were consistent with dissociation of IgG-antigen complexes from gE-gI upon trafficking to acidic intracellular vesicles. In contrast, the gp68-Fc interaction is broadly stable across acidic and basic pHs (17), suggesting a potentially different intracellular trafficking pathway if gp68, like gE-gI, can internalize ABB complexes.

To investigate ABB mediated by HCMV gp68, we adapted the model system used to characterize gE-gI-mediated ABB (8). In the gE-gI studies, we transiently expressed gE-gI and gD in HeLa cells and then investigated the trafficking of gE-gI and gD under ABB and non-ABB conditions (8). We chose gD as the model antigen because it is a cell surface glycoprotein found on virions and infected cells (18), and fusion of its cytoplasmic tail to a fluorescent protein did not affect cellular distribution or transport (19). We showed that a gD-Dendra2 fusion protein localized primarily to the cell surface in the presence or absence of an anti-gD antibody under non-ABB conditions (8); thus, we could use this protein to investigate the fate of a cell surface antigen under ABB conditions. We used an anti-gD IgG antibody (20) with a human Fc (anti-gD$_{hFc}$) that can bind to gE-gI and to gD to create ABB complexes and two types of control IgGs to create non-ABB complexes: the anti-gD antibody fused with a mouse Fc (anti-gD$_{mFc}$), which binds gD, but not gE-gI; and a human IgG against an unrelated antigen (IgG$_{hFc}$), which binds gE-gI, but not gD (Fig. 1). These IgGs were expressed in mammalian cells as described previously (8). We found that gD expressed in gE-gI-positive cells was internalized together with anti-gD$_{hFc}$, but it remained at the cell surface when cells were incubated with anti-gD$_{mFc}$ or IgG$_{hFc}$ (8).

For the gp68 ABB system, we expressed gp68 together with the gD-Dendra2 fusion protein using a previously described bicistronic construct (8). For control experiments, we also expressed untagged gp68 alone and as a gp68-Dendra2 fusion protein. Three-dimensional (3D) imaging of fixed cells expressing untagged gp68 or gp68-Dendra2 showed comparable levels and localization of both proteins in experiments using labeled anti-gD$_{hFc}$ (Fig. 2A) and gp68-Dendra2 colocalized with IgG$_{hFc}$ in intracellular compartments (Fig. 3A); thus, the introduction of
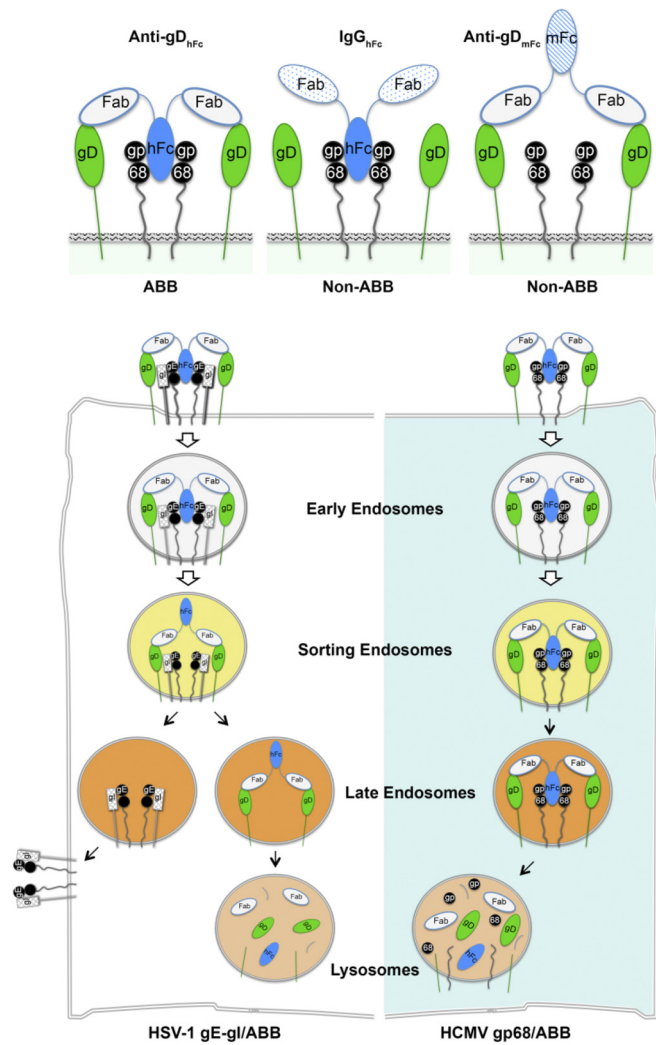
FIG 1 Schematic diagrams of ABB and non-ABB complexes at a cell surface and comparison of intracellular trafficking of gE-gI- and gp68-mediated ABB complexes. (Top) ABB complex containing gp68, anti-gD$_{hFc}$, and gD (left) and non-ABB complexes containing IgG$_{hFc}$ bound to gp68, but not gD (middle), and anti-gD$_{mFc}$ bound to gD, but not gp68 (right). (Bottom) Proposed pathways for intracellular trafficking of ABB complexes. Cell surface ABB complexes are internalized through endocytosis into early endosomes and sorting endosomes. Upon acidification, the Fabs remain bound to gD, and the Fc region of anti-gD$_{hFc}$ dissociates from HSV1-gE-gI, but not from HCMV gp68. The IgG-gD complex internalized with gE-gI, and the IgG-gD-gp68 complex then traffics to degradative lysosomes, allowing free gE-gI, but not gp68, to be recycled back to the cell surface.

the C-terminal tag did not detectably affect Fc binding or the gp68 cellular distribution. Cells expressing gp68-Dendra2 bound anti-gD$_{hFc}$ and IgG$_{hFc}$, but not anti-gD$_{mFc}$ (Fig. 2B), consistent with previous reports that cells infected with wild-type HCMV bind human, but not mouse, IgG (21). Together with previous demonstrations that both anti-gD$_{hFc}$ and anti-gD$_{mFc}$ bind gD (8), these results showed that the three forms of IgG could be used to create ABB or non-ABB conditions when gp68 was coexpressed with gD.

We next conducted internalization experiments using cells coexpressing gp68 and gD under ABB and non-ABB conditions (Fig. 1). Cells transiently expressing gp68 and gD-Dendra2 were incu-

bated with fluorescently labeled IgGs (anti-gD$_{hFc}$, anti-gD$_{mFc}$, or IgG$_{hFc}$) and then stained with CellMask, a plasma membrane marker. As expected, the gp68-binding IgGs anti-gD$_{hFc}$ and IgG$_{hFc}$ were internalized after incubation with the cells, whereas anti-gD$_{mFc}$ remained at the cell surface, where it colocalized with gD and the membrane marker (Fig. 2C). gD remained at the cell surface when cells were incubated with either anti-gD$_{mFc}$ or IgG$_{hFc}$, as demonstrated by colocalization with CellMask at the plasma membrane, but was internalized when cells were incubated with anti-gD$_{hFc}$ (Fig. 2C and D). Thus, as previously found for the gE-gI studies (8), gD was internalized through indirect interactions with the receptor as an IgG-antigen complex under ABB conditions, whereas when the IgG bound only to gD (anti-gD$_{mFc}$) or the viral FcγR (IgG$_{hFc}$), gD remained at the cell surface.

We performed live-cell four-dimensional (4D) confocal imaging to follow the intracellular trafficking of ABB complex components using labeled epidermal growth factor (EGF) as a lysosomal marker. EGF binds its cell surface receptor prior to being internalized and transported through the acidic environment of early endosomes, multivesicular bodies/late endosomes, and lysosomes (22–25). HeLa cells expressing gp68 and gD-Dendra2 were coincubated with fluorescently labeled EGF and a labeled version of either anti-gD$_{hFc}$, IgG$_{hFc}$, or anti-gD$_{mFc}$. At early time points in samples incubated with anti-gD$_{hFc}$, gD, and EGF, anti-gD$_{hFc}$ fluorescence was primarily localized at the cell surface, and the small amount of intracellular gD and anti-gD$_{hFc}$ fluorescence was not found in EGF-positive compartments. At later time points, increasing numbers of triple-positive intracellular vesicles staining for EGF, gD, and anti-gD$_{hFc}$ were observed (Fig. 3B to D; see Movie S1 in the supplemental material). These results are consistent with a model in which gp68–anti-gD$_{hFc}$–gD ABB complexes are internalized into endosomes and remain associated at low pH such that they traffic together into EGF-positive lysosomes (Fig. 1). Under non-ABB conditions, gD fluorescence remained predominantly at the cell surface at all time points in gp68/gD-positive cells treated with either IgG$_{hFc}$ or anti-gD$_{mFc}$ (Fig. 3B to D; see Movies S2 and S3 in the supplemental material). Internalized IgG$_{hFc}$ fluorescence was found mainly in EGF-negative compartments at early time points (10 min) and then in EGF-positive compartments at later time points (60 min). Statistical analyses of pairwise 3D colocalization as a function of time (Fig. 3C) demonstrated colocalization of gD with the two anti-gD antibodies, but not with IgG$_{hFc}$, at time points after 10 min, as expected since only the anti-gD antibodies bind to gD throughout the experiment (Fig. 3C and D). When incubated with anti-gD$_{hFc}$, gD became increasingly more colocalized with EGF and anti-gD$_{hFc}$, whereas when incubated with IgG$_{hFc}$, EGF colocalized with IgG$_{hFc}$, but not gD, at later time points. When incubated with anti-gD$_{mFc}$, gD did not colocalize with EGF. These results demonstrated that cell surface gD was exclusively internalized and targeted into EGF-positive lysosomes under ABB conditions, consistent with a model in which gp68–anti-gD$_{hFc}$–gD ABB complexes and gp68-IgG$_{hFc}$ complexes are internalized into endosomal vesicles and remain associated at low pH such that they traffic together into EGF-positive lysosomes, whereas anti-gD$_{mFc}$ remained attached to cell surface gD because it did not bind to gp68. We repeated the internalization experiments in fixed cells using LAMP2A as a lysosomal marker (26). Cells expressing gp68 and gD-Dendra2 were incubated for 2 h with labeled anti-gD$_{hFc}$, IgG$_{hFc}$, or anti-gD$_{mFc}$,
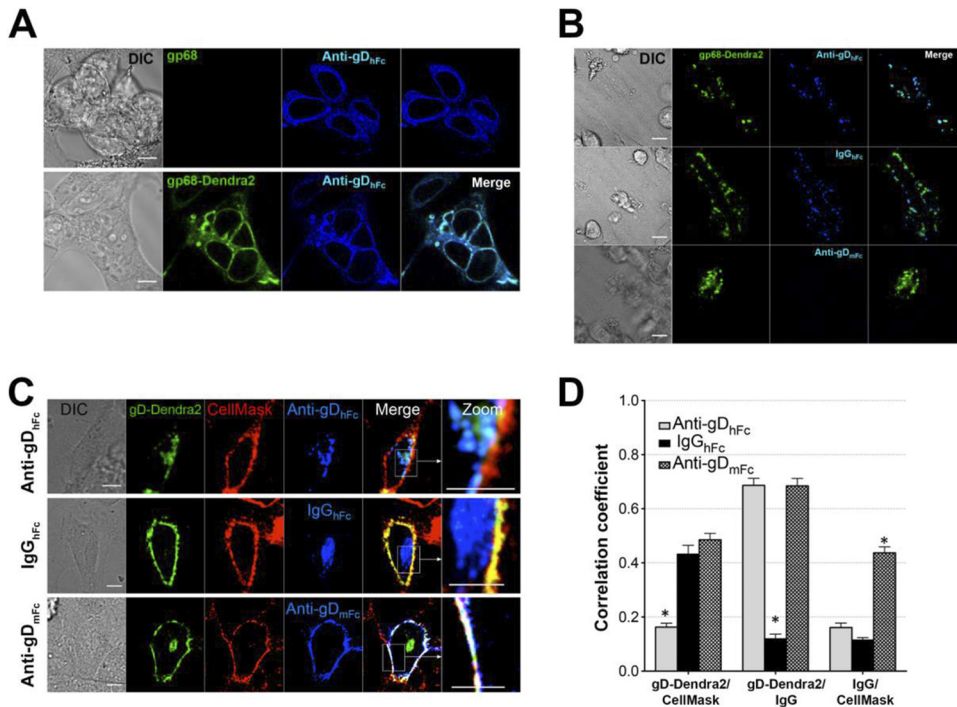
FIG 2 Characterization of components of the ABB model system. Scale bars, 10 μm. (A) Demonstration that gp68 and gp68-Dendra2 localize similarly in transfected cells. HeLa cells transiently expressing gp68 or gp68 tagged with Dendra2 fluorescent protein (gp68-Dendra2) were fixed in 4% paraformaldehyde (PFA) and incubated with AF647-labeled anti-gD$_{hFc}$. IgGs were labeled to similar degrees using the Alexa Fluor 647 protein labeling kit following the instructions in the manufacturer's protocol (https://tools.thermofisher.com/content/sfs/manuals/mp20173.pdf). The localizations of gp68 and gp68-Dendra2 were similar, suggesting that both bound human Fc and fusion of Dendra2 to the gp68 cytoplasmic tail did not alter trafficking. (B) Demonstration that gp68 binds human IgG Fc (top and middle panels), but not mouse IgG Fc (bottom). HeLa cells transiently expressing gp68-Dendra2 were incubated with AF647-labeled anti-gD$_{hFc}$, IgG$_{hFc}$, or anti-gD$_{mFc}$ for 30 min at 37°C under a 5% CO$_2$ atmosphere and fixed as described for panel A. (C and D) Internalization of gD and IgG under ABB-permissive and nonpermissive conditions. HeLa cells coexpressing gp68 (nontagged) and gD-Dendra2 (green) were pulsed with AF647-labeled IgGs (blue) for 60 min and then treated with AF555-labeled CellMask (red), a plasma membrane marker, for 5 min at 37°C under a 5% CO$_2$ atmosphere. Samples were rinsed to remove excess dye, and 3D imaging (0.5- to 1-μm section thickness and up to 16-μm total depth) was performed using a 63× objective (αPlan-ApoChromat 1.45 oil differential inference contrast [DIC]) and an electron-multiplying charge-coupled device camera (Hamamatsu Photonics) guided by Volocity software on a Perkin-Elmer spinning-disk confocal microscope. (C) Representative confocal slices from cells treated with anti-gD$_{hFc}$, IgG$_{hFc}$, or anti-gD$_{mFc}$. Regions of gD-IgG colocalization appear cyan, regions of CellMask-gD colocalization appear yellow, regions of CellMask-IgG colocalization appear magenta, and regions of triple colocalization (CellMask-gD-IgG) appear white. Experiments were repeated at least three times with analyses of ≥30 cells. (D) 3D thresholded Pearson correlation coefficient analyses for data from ≥30 cells. Correlation coefficients are presented as the mean and standard deviation from experiments repeated at least three times. Asterisks indicate a significant difference of colocalization compared to other members in the same category ($P < 0.01$).

immunostained with anti-LAMP2A, and 3D confocal imaging and statistical analyses of pairwise colocalizations were performed. Consistent with lysosomal routing of ABB complexes, cells incubated with anti-gD$_{hFc}$ showed three pairwise colocalizations (gD with anti-gD$_{hFc}$, gD with LAMP2A, and anti-gD$_{hFc}$ with LAMP2A), cells incubated with IgG$_{hFc}$ showed single colocalization (IgG$_{hFc}$ with LAMP2A), and cells incubated with anti-gD$_{mFc}$ also showed single colocalization (gD with anti-gD$_{mFc}$) (Fig. 4).

Here we investigated the fate of HCMV gp68-mediated ABB complexes using techniques developed for studying ABB mediated by HSV-1 gE-gI (8). We found that, like gE-gI, gp68 formed ABB complexes with anti-gD$_{hFc}$ and gD, resulting in internalization of gD. The internalization required gp68-mediated ABB, since it occurred only in the presence of the IgG that could bind to both gp68 and gD, but not in the presence of the anti-gD$_{mFc}$ and IgG$_{hFc}$ control antibodies. However, the ABB complexes formed with gp68, IgG, and gD apparently did not dissociate after endo-

cytosis; instead all three components were trafficked to lysosomes, where they were presumably degraded (Fig. 1). Extrapolation of these results to virally infected cells provides a mechanism by which infected cells can sequester both host antiviral antibodies and their viral antigen targets from the host immune system by targeting them for degradation in lysosomes. In the case of HCMV gp68, the cotrafficking of the viral FcγR to lysosomes together with the IgG-antigen complex should also result in degradation of the receptor, whereas dissociation of gE-gI from the IgG-antigen complex prior to entering lysosomes would allow gE-gI to be recycled back to the cell surface. The postulated differences in trafficking resulting in degradation of gp68, but not gE-gI, may reflect the fact that HCMV expresses at least three different IgG Fc binding proteins (3, 13, 14), compared with HSV-1, which expresses only one known FcγR (5, 11). For both viruses, internalization of ABB complexes and consequent degradation would enable clearance of membrane proteins that serve as antigenic targets and selective removal of antiviral antibodies,
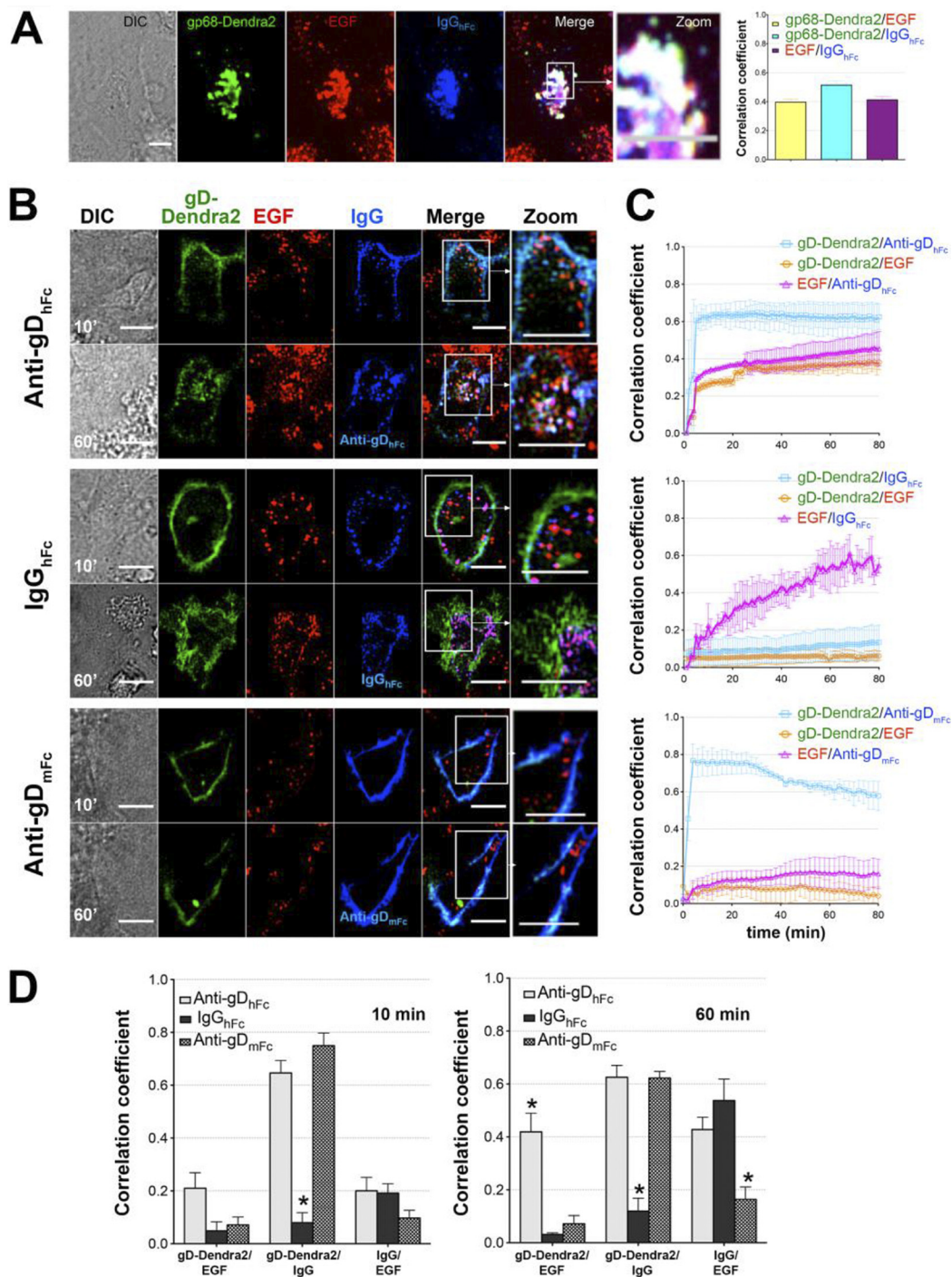
FIG 3 Colocalization of gD and IgG with EGF under ABB-permissive and nonpermissive conditions. (A) Demonstration in fixed cells that gp68-Dendra2/IgG$_{hFc}$ complexes traffic into lysosomes under non-ABB conditions. HeLa cells expressing gp68-Dendra2 (green) were incubated at 37°C under a 5% CO_2 atmosphere with AF568-labeled EGF (red) for 30 min and then with AF647-labeled IgG$_{hFc}$ (blue). Confocal z-stacks were captured with a 63×, NA 1.4 objective on a PerkinElmer spinning-disk confocal microscope after 30 min. Regions of gp68-Dendra2/IgG$_{hFc}$ colocalization appear cyan, and regions of EGF/gp68-Dendra2/IgG$_{hFc}$ triple colocalization appear white. Histograms show the 3D thresholded Pearson correlation coefficient analyses for data from ≥30 cells that showed positive colocalization levels between gp68-Dendra2, IgG$_{hFc}$ and EGF above a background level of 2%. (B to D) For live cell imaging experiments, HeLa cells coexpressing gp68 and gD-Dendra2 (green) were incubated for 30 min with 50 nM AF568-conjugated EGF (red) in L15 medium at 37°C and a 5% CO_2 atmosphere. Samples in coverglass bottom dishes (Thermo Scientific/Nunc) were rinsed to remove excess dye. After imaging an initial z-stack (as described in Fig. 2), AF647-conjugated anti-gD$_{mFc}$, anti-gD$_{hFc}$, or IgG$_{hFc}$ (blue) was added to a final concentration of 2 µg/ml, and multichannel z-stacks were captured approximately every 1 to 3 min for at least 1 h. (B) Representative confocal slices from early (10-min) and late (60-min) time points. Regions of gD-IgG colocalization appear cyan, regions of EGF-IgG colocalization appear magenta, and regions of triple colocalization appear white. Three independent experiments were performed, each with analysis of ≥5 live cells. Scale bar, 10 µm. (C) 4D thresholded Pearson correlation coefficient analyses (presented for each condition as the mean and standard deviation) for data from ≥5 live cells in three independent experiments. HeLa cells expressing gp68 and gD-Dendra2 were incubated with AF568-labeled EGF and either AF647-labeled anti-gD$_{hFc}$ (top panel), IgG$_{hFc}$ (middle panel), or anti-gD$_{mFc}$ (bottom panel). Correlation coefficients are shown for gD versus IgG (cyan curve, open squares), gD versus EGF (orange curve, open circles), and EGF versus IgG (magenta curve, open triangles). (D) Histograms comparing correlations at 10 min (left) and 60 min (right) time points. Asterisks indicate a significant difference of colocalization compared to other members in the same category ($P < 0.05$).
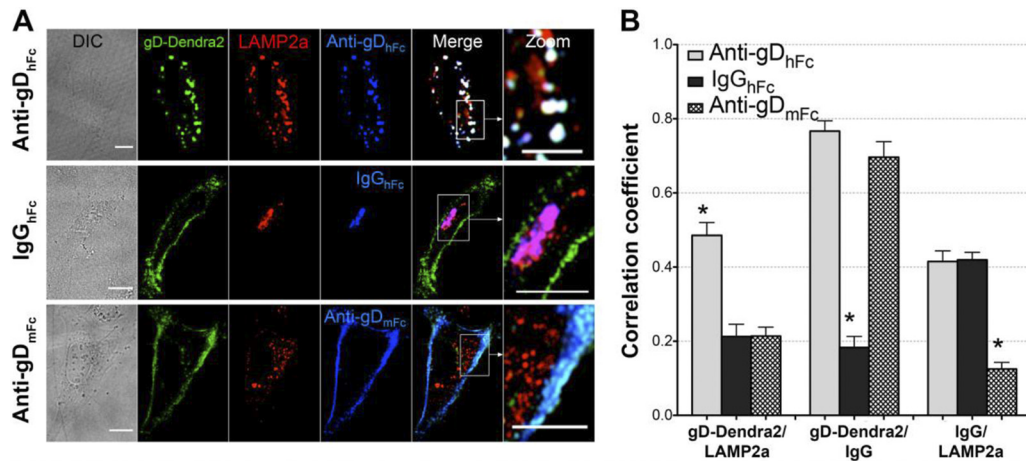
FIG 4 Colocalization of gD and IgG with LAMP2A under ABB permissive and nonpermissive conditions. (A) Confocal slices of HeLa cells transiently expressing gp68 and gD-Dendra2 (green) and incubated for 2 h at 37°C under a 5% CO_2 atmosphere with one of the three AF647-labeled IgGs (blue): anti-gD$_{hFc}$ (top), IgG$_{hFc}$ (middle), or anti-gD$_{mFc}$ (bottom). After fixation in 4% paraformaldehyde, cells were stained with AF568-labeled anti-LAMP2A (red). Regions of red (LAMP2A) and green (gD) colocalization appear yellow, regions of red (LAMP2A) and blue (IgG) colocalization appear purple, regions of green (gD) and blue (IgG) colocalization appear cyan, and regions of red (LAMP2A), green (gD), and blue (IgG) colocalization appear white. (B) Histograms comparing correlations at the 10-min (left) and 60-min (right) time points. Asterisks indicate a significant difference of colocalization compared to those of other members in the same category ($P < 0.05$).

thereby allowing these viruses to evade IgG-mediated immune effector functions.

REFERENCES

1. **Nogalski MT, Collins-McMillen D, Yurochko AD.** 2014. Overview of human cytomegalovirus pathogenesis. Methods Mol Biol **1119:**15–28. http://dx.doi.org/10.1007/978-1-62703-788-4_2.
2. **Crough T, Khanna R.** 2009. Immunobiology of human cytomegalovirus: from bench to bedside. Clin Microbiol Rev **22:**76–98. http://dx.doi.org/10.1128/CMR.00034-08.
3. **Atalay R, Zimmermann A, Wagner M, Borst E, Benz C, Messerle M, Hengel H.** 2002. Identification and expression of human cytomegalovirus transcription units coding for two distinct Fcgamma receptor homologs. J Virol **76:**8596–8608. http://dx.doi.org/10.1128/JVI.76.17.8596-8608.2002.
4. **Dubin G, Frank I, Friedman HM.** 1990. Herpes simplex virus type 1 encodes two Fc receptors which have different binding characteristics for monomeric immunoglobulin G (IgG) and IgG complexes. J Virol **64:**2725–2731.
5. **Johnson DC, Frame MC, Ligas MW, Cross AM, Stow ND.** 1988. Herpes simplex virus immunoglobulin G Fc receptor activity depends on a complex of two viral glycoproteins, gE and gI. J Virol **62:**1347–1354.
6. **Lilley BN, Ploegh HL, Tirabassi RS.** 2001. Human cytomegalovirus open reading frame TRL11/IRL11 encodes an immunoglobulin G Fc-binding protein. J Virol **75:**11218–11221. http://dx.doi.org/10.1128/JVI.75.22.11218-11221.2001.
7. **Dubin G, Socolof E, Frank I, Friedman HM.** 1991. Herpes simplex virus type 1 Fc receptor protects infected cells from antibody-dependent cellular cytotoxicity. J Virol **65:**7046–7050.
8. **Ndjamen B, Farley AH, Lee T, Fraser SE, Bjorkman PJ.** 2014. The herpes virus Fc receptor gE-gI mediates antibody bipolar bridging to clear viral antigens from the cell surface. PLoS Pathog **10:**e1003961. http://dx.doi.org/10.1371/journal.ppat.1003961.
9. **Sprague ER, Wang C, Baker D, Bjorkman PJ.** 2006. Crystal structure of the HSV-1 Fc receptor bound to Fc reveals a mechanism for antibody bipolar bridging. PLoS Biol **4:**e148. http://dx.doi.org/10.1371/journal.pbio.0040148.
10. **Frank I, Friedman HM.** 1989. A novel function of the herpes simplex virus type 1 Fc receptor: participation in bipolar bridging of antiviral immunoglobulin G. J Virol **63:**4479–4488.
11. **Lubinski JM, Lazear HM, Awasthi S, Wang F, Friedman HM.** 2011. The herpes simplex virus 1 IgG Fc receptor blocks antibody-mediated complement activation and antibody-dependent cellular cytotoxicity in vivo. J Virol **85:**3239–3249. http://dx.doi.org/10.1128/JVI.02509-10.
12. **Van Vliet KE, De Graaf-Miltenburg LA, Verhoef J, Van Strijp JA.** 1992. Direct evidence for antibody bipolar bridging on herpes simplex virus-infected cells. Immunology **77:**109–115.
13. **Corrales-Aguilar E, Hoffmann K, Hengel H.** 2014. CMV-encoded Fcγ receptors: modulators at the interface of innate and adaptive immunity. Semin Immunopathol **36:**627–640. http://dx.doi.org/10.1007/s00281-014-0448-2.
14. **Cortese M, Calò S, D'Aurizio R, Lilja A, Pacchiani N, Merola M.** 2012. Recombinant human cytomegalovirus (HCMV) RL13 binds human immunoglobulin G Fc. PLoS One **7:**e50166. http://dx.doi.org/10.1371/journal.pone.0050166.
15. **Corrales-Aguilar E, Trilling M, Hunold K, Fiedler M, Le VT, Reinhard**

H, Ehrhardt K, Mercé-Maldonado E, Aliyev E, Zimmermann A, Johnson DC, Hengel H. 2014. Human cytomegalovirus Fcγ binding proteins gp34 and gp68 antagonize Fcγ receptors I, II and III. PLoS Pathog 10: e1004131. http://dx.doi.org/10.1371/journal.ppat.1004131.

16. Sprague ER, Martin WL, Bjorkman PJ. 2004. pH dependence and stoichiometry of binding to the Fc region of IgG by the herpes simplex virus Fc receptor gE-gI. J Biol Chem 279:14184–14193. http://dx.doi.org/10.1074/jbc.M313281200.

17. Sprague ER, Reinhard H, Cheung EJ, Farley AH, Trujillo RD, Hengel H, Bjorkman PJ. 2008. The human cytomegalovirus Fc receptor gp68 binds the Fc C_H2-C_H3 interface of immunoglobulin G. J Virol 82:3490–3499. http://dx.doi.org/10.1128/JVI.01476-07.

18. Norrild B, Virtanen I, Lehto VP, Pedersen B. 1983. Accumulation of herpes simplex virus type 1 glycoprotein D in adhesion areas of infected cells. J Gen Virol 64:2499–2503. http://dx.doi.org/10.1099/0022-1317-64-11-2499.

19. Snyder A, Bruun B, Browne HM, Johnson DC. 2007. A herpes simplex virus gD-YFP fusion glycoprotein is transported separately from viral capsids in neuronal axons. J Virol 81:8337–8340. http://dx.doi.org/10.1128/JVI.00520-07.

20. Mayfield SP, Franklin SE, Lerner RA. 2003. Expression and assembly of a fully active antibody in algae. Proc Natl Acad Sci U S A 100:438–442. http://dx.doi.org/10.1073/pnas.0237108100.

21. Antonsson A, Johansson PJ. 2001. Binding of human and animal immunoglobulins to the IgG Fc receptor induced by human cytomegalovirus. J Gen Virol 82:1137–1145. http://dx.doi.org/10.1099/0022-1317-82-5-1137.

22. Haigler HT, McKanna JA, Cohen S. 1979. Direct visualization of the binding and internalization of a ferritin conjugate of epidermal growth factor in human carcinoma cells A-431. J Cell Biol 81:382–395. http://dx.doi.org/10.1083/jcb.81.2.382.

23. Futter CE, Pearse A, Hewlett LJ, Hopkins CR. 1996. Multivesicular endosomes containing internalized EGF-EGF receptor complexes mature and then fuse directly with lysosomes. J Cell Biol 132:1011–1023. http://dx.doi.org/10.1083/jcb.132.6.1011.

24. Clague MJ, Urbé S. 2001. The interface of receptor trafficking and signalling. J Cell Sci 114:3075–3081.

25. Haglund K, Di Fiore PP, Dikic I. 2003. Distinct monoubiquitin signals in receptor endocytosis. Trends Biochem Sci 28:598–603. http://dx.doi.org/10.1016/j.tibs.2003.09.005.

26. Ndjamen B, Kang BH, Hatsuzawa K, Kima PE. 2010. Leishmania parasitophorous vacuoles interact continuously with the host cell's endoplasmic reticulum; parasitophorous vacuoles are hybrid compartments. Cell Microbiol 12:1480–1494. http://dx.doi.org/10.1111/j.1462-5822.2010.01483.x.